Thieme

Two *Olea europaea* L. Extracts Reduce Harmful Effects in a Model of Neurotoxicity: Involvement of the Endoplasmic Reticulum

OPEN ACCESS

Authors

Jessica Maiuolo[1]*, Sonia Bonacci[1]*, Francesca Bosco[2], Lorenza Guarnieri[2], Stefano Ruga[2], Antonio Leo[2,3], Rita Citraro[2,3], Salvatore Ragusa[4], Ernesto Palma[1], Vincenzo Mollace[1], Giovambattista De Sarro[2,3]

Affiliations

1 Department of Health Sciences, School of Pharmacy, Magna Graecia University of Catanzaro, Catanzaro, Italy
2 Department of Health Science, School of Medicine and Surgery, Magna Graecia University of Catanzaro, Catanzaro, Italy
3 System and Applied Pharmacology@University Magna Grecia, Science of Health Department, School of Medicine, Magna Graecia University of Catanzaro, Catanzaro, Italy
4 PLANTA/Research, Documentation and Training Center, Palermo, Italy

Keywords

Olea europaea, Oleaceae, endoplasmic reticulum, oxidative damage, neurons, lead

received March 18, 2024
accepted after revision June 10, 2024

Bibliography

Planta Med 2024
DOI 10.1055/a-2353-1469
ISSN 0032-0943

Georg Thieme Verlag KG, Rüdigerstraße 14,
70469 Stuttgart, Germany

Correspondence

Dr. Jessica Maiuolo
Campus Germaneto, Department of Health Sciences, Magna Graecia University of Catanzaro
Viale Europa, 88100 Catanzaro, Italy
Phone: + 39 (0) 96 13 69 51 23
maiuolo@unicz.it

ABSTRACT

Prolonged exposure to lead has been recognized as harmful to human health as it may cause neurotoxic effects including mitochondrial damage, apoptosis, excitotoxicity, and myelin formation alterations, among others. Numerous data have shown that consuming olive oil and its valuable components could reduce neurotoxicity and degenerative conditions. Olive oil is traditionally obtained from olive trees; this plant (*Olea europaea* L.) is an evergreen fruit tree.

In this manuscript, two extracts have been used and compared: the extract from the leaves of *Olea europaea* L. (OE) and the extract derived from OE but with a further sonication process (s-OE). Therefore, the objectives of this experimental work were as follows: 1) to generate an innovative extract; 2) to test both extracts on a model of neurotoxicity of human neurons induced following lead exposure; and 3) to study the mechanisms behind lead-induced neurotoxicity.

The results showed that the mechanism involved in the neurotoxicity of lead included dysfunction of the cellular endoplasmic reticulum, which suffered oxidative damage. In addition, in all experiments, s-OE was more effective than OE, having greater and better effects against lead-induced damage and being dissolved in a smaller amount of EtOH, which promotes its sustainability.

Introduction

Neurotoxicity indicates adverse effects that affect the nervous system and that result from exposure to potentially toxic substances [1]. Environmental pollution has increased daily exposure to often harmful chemicals such as metals, solvents, pesticides, and other contaminants [2]. Among these, heavy metals easily spread in the food chain, leading to alterations of biological macromolecules such as DNA, proteins, and lipids [3]. The accumulation of heavy metals can cause damage to the nervous system: some metals can cross the blood–brain barrier, reach the central nervous system, and cause neurotoxicity or neurodegeneration. Many of these metals have been linked to devastating neurologi-

* These authors contributed equally to this work

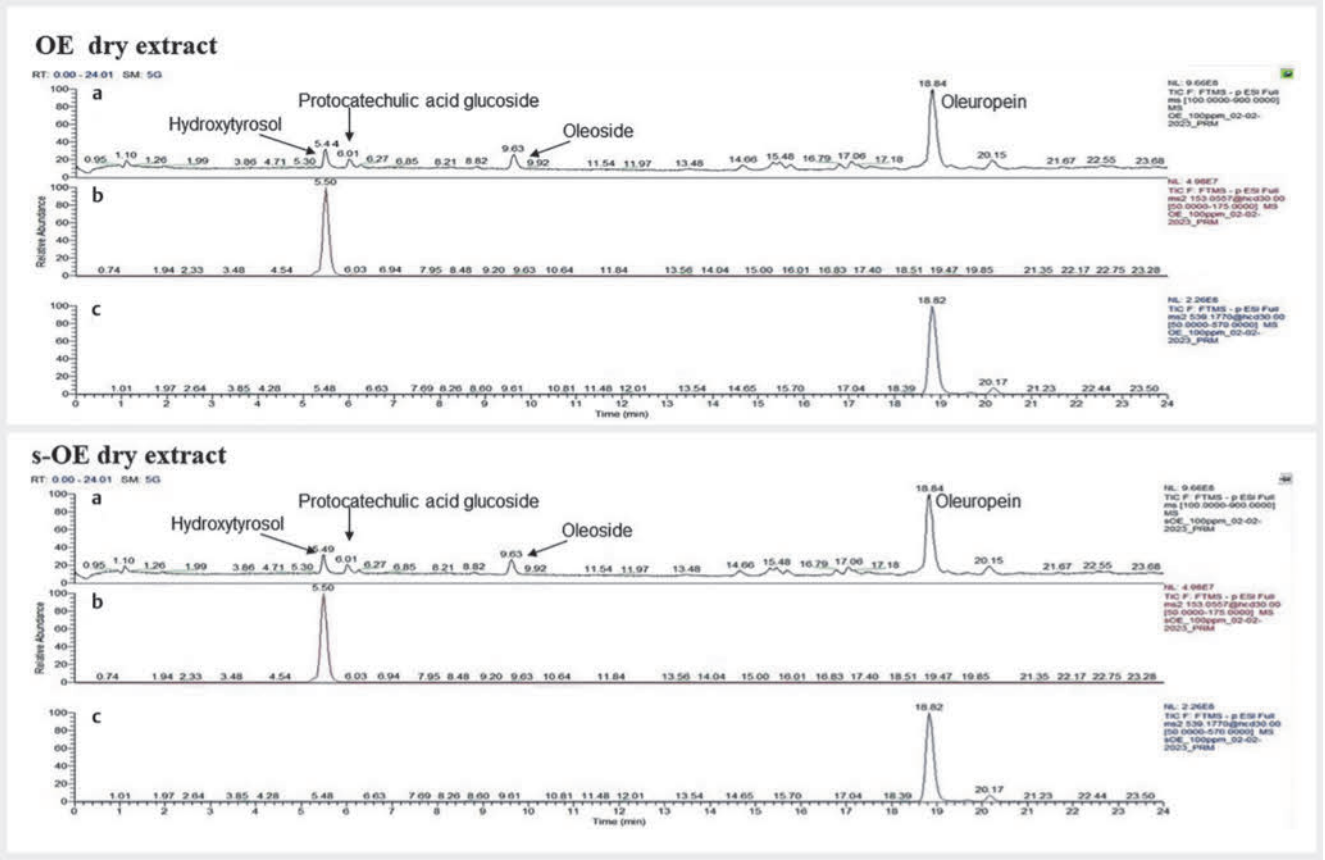

▶ **Fig. 1** LC-HRMS full-scan chromatogram (a) and LC-HRMS PRM chromatograms of (**b**) hydroxytyrosol and (**c**) oleuropein in OE and s-OE dry extracts.

cal disorders, such as mental retardation [4], Alzheimer's disease [5], Parkinson's disease [6], multiple sclerosis [7], and amyotrophic lateral sclerosis [8]. Lead (Pb) is present in trace amounts in soil, plants, and water; anthropic activity is responsible for the increased exposure to lead. Chemically, the lead diffused in the environment is in the oxidation state + 2 (Pb^{2+}), and its accumulation occurs due to its inability to degrade and its subsequent absorption into the soil [9, 10]. Prolonged exposure to lead can cause a variety of health disorders [11].

Numerous data in the literature have shown that consuming olive oil and its valuable components could reduce neurotoxicity and degenerative conditions [12]. Olive oil has a predominant role in the prevention of chronic and/or degenerative diseases, demonstrating antioxidant, anti-inflammatory, anti-obesity, anti-diabetic, cardioprotective, antisteatotic, anticancer, antimicrobial, and neuroprotective effects [13]; 98–99% of olive oil (saponifiable fraction) consists of monounsaturated fatty acids (MUFA), polyunsaturated acids (PUFA), and short-chain saturated fats (SFA). The remaining 1–2% (unsaponifiable fraction) includes sterols, pigments, aliphatic alcohols, tocopherols (vitamin E), squalene, terpenoids, and phenolic compounds [14]. These latter are characterized by a broad spectrum of beneficial effects on human health [15], and the most present in olive oil are oleuropein, hydroxytyrosol, and oleacein. Oleuropein is an ester of elenolic acid and belongs to the family of secoiridoids; its degradation leads to the formation of two dialdehydic-form molecules: 3,4-DHPEA-EDA (oleacein) and 3,4-DHPEA (hydroxytyrosol) [16]. Oleuropein and hydroxytyrosol have been extensively studied, and their antioxidant effect is particularly recognized; while initially, less attention has been given to oleacein, it is the most abundant secoiridoid in the fruit and leaves of olive trees. To date, knowledge about oleacein has greatly increased, and there are numerous data available in the literature on this subject. Oleacein plays an important anti-proliferative and anti-metastatic role, as demonstrated by an interesting study conducted precisely on the SH-SY5Y cell line [17]. This study showed that oleacein can exercise important anti-cancer effects, reducing cell proliferation, by blocking the cell cycle in the S phase and inducing apoptotic death through increased expression of Bax and p53. In addition, oleacein exerts an important anti-inflammatory activity [18], being thus a possible alternative pharmacological strategy against cancer and inflammation. The traditional method of obtaining extra-virgin olive oil is its extraction from olives, the fruit of the olive tree. This plant (*Olea europaea* L.) is an evergreen fruit tree belonging to the Oleaceae family and the genus *Olea*. The olive tree is a typically thermophilic and heliophilous plant, initially cultivated almost exclusively in the Mediterranean countries with mild winters and warm summers, although later it was successfully planted also in

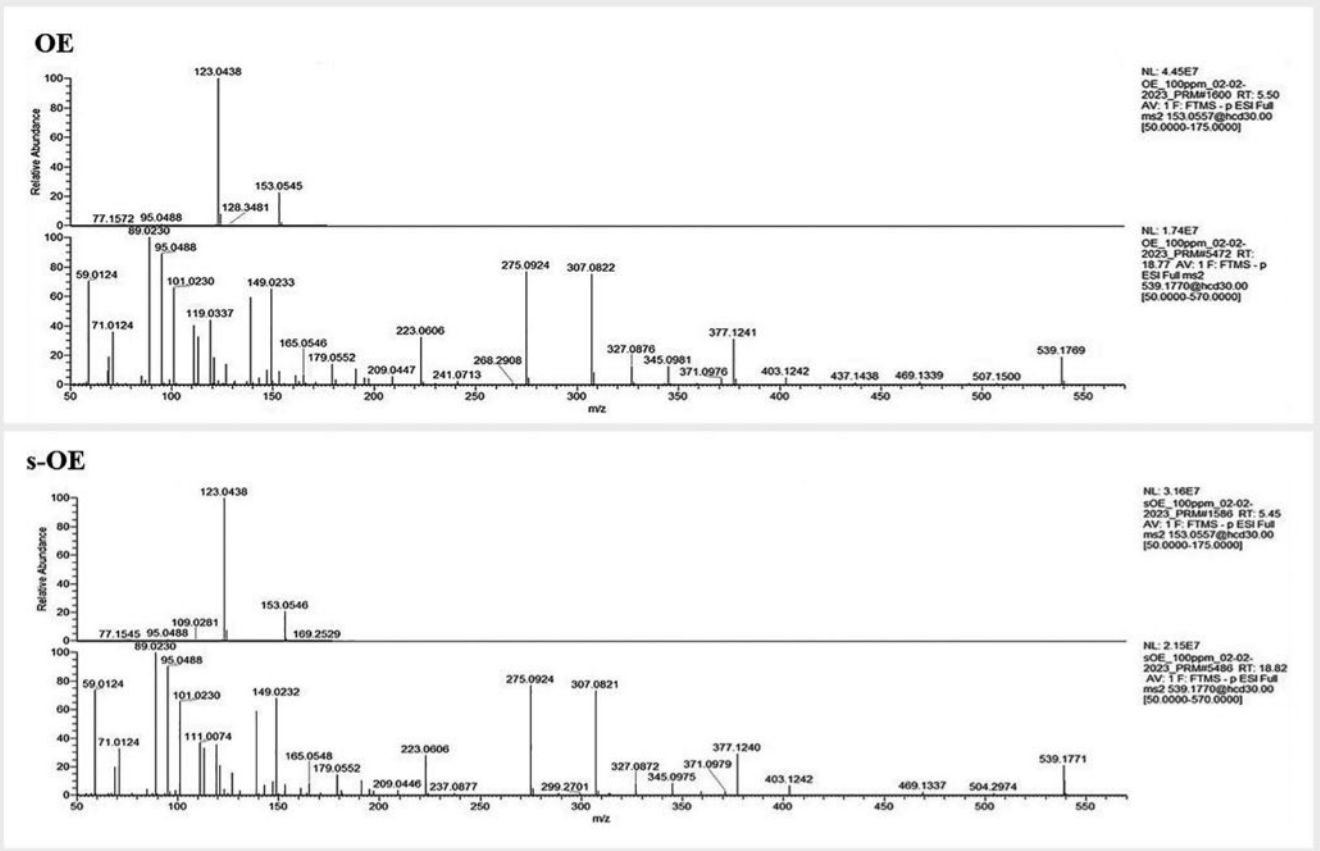

▶ **Fig. 2** MSMS spectra of (**a**) hydroxytyrosol (153.0557 m/z) and (**b**) oleuropein (539.1170 m/z) in OE and s-OE extracts.

other countries with similar climates, such as Australia, Argentina, California, South Africa, and New Zealand. To date, the five countries with the largest olive-growing areas are Spain, Greece, Italy, Tunisia, and Turkey. The fruit is a yellow-green to black-purple drupe, formed by a "fleshy" part (pulp that contains oil) and by the woody core containing the seed. From the pressing and crushing of olives comes olive oil [19, 20]: the processing of olive oil generates different types of waste such as leaves and branches from tree pruning, solid waste from the mill, wastewater from oil mills, and olive kernels. In recent years, the trend has been to develop energy or economic gain from these wastes [21]. For example, olive leaves are characterized by a very rich composition that includes natural bioactive and phenolic compounds, which possess a health promotion potential. The organic matter of olive leaves is variable and represents about 38% of their weight [22–25]. The amount of polyphenols in olive leaves is higher than that of olive oil (15–70 mg/g fresh weight) [26–29].

In this manuscript, two extracts have been used and compared: a) the extract from the leaves of *Olea europaea* L, cultivar Coratina, (OE); b) the extract obtained from OE and derived from a further sonication process (s-OE). Most drugs used to ensure an adequate therapeutic response against various pathological conditions are characterized by poor aqueous solubility that reduces bioavailability. This phenomenon is also demonstrated in herbal medicines [30]. The protocol developed to obtain an extract from the leaves of *Olea Europaea* provides for its final dissolution in a hydroalcoholic solution consisting of water and ethanol (30:70) [31, 32]. Since ethanol could be toxic if taken in high concentrations, it would be desirable to reduce the amount of alcohol and still ensure its dissolution. For this reason, in this experimental study, we subjected the extract to a sonication process, which improved its dissolution, allowing it to reduce the amount of ethanol in the hydroalcoholic solution used.

Therefore, the objectives of this experimental work were as follows:

1. Generate an innovative extract (s-OE);
2. Test both extracts (OE and s-OE) on an *in vitro* model of neurotoxicity induced in human neurons following lead exposure;
3. Study the mechanisms underlying the effects generated by lead to interpret the action of OE and s-OE extracts correctly.

Results

Hydroxytyrosol and oleuropein in OE and s-OE

As can be seen in ▶ **Fig. 1** and **Fig. 2**, the concentrations of hydroxytyrosol and oleuropein are the same in both OE and s-OE and represent, respectively, 6.38% and 42.17% w/w of the extracts.

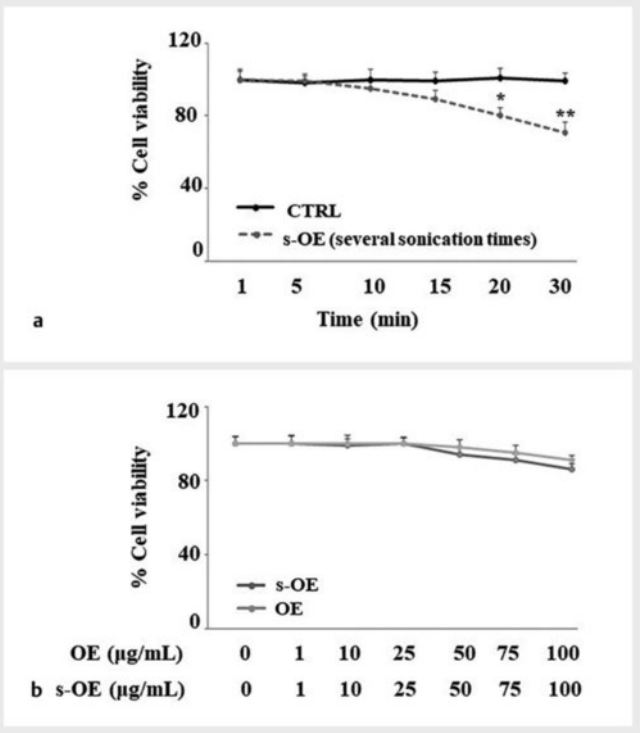

▶ **Fig. 3** Experiments of cell viability. In panel **a**, the OE extract was subjected to different sonication times, and its viability values were obtained. In panel **b**, the effects of OE and s-OE on cell viability were compared. Three independent experiments were carried out, and the values are expressed as the mean ± standard deviation (sd). * denotes $p < 0.05$ vs. CTRL; ** denotes $p < 0.01$ vs. CTRL. The Student test was applied.

s-OE preparation

s-OE extract was produced using sonication and the best sonication time was established by specific viability experiments, in which OE was sonicated for a different duration of time (▶ **Fig. 3a**). Since the sonication time of 10′ did not cause changes in cell viability compared to untreated cells, we chose this time to get s-OE. The viability of cells treated with OE or s-OE is indicated in ▶ **Fig. 3b**: no significant variation was found, and we chose to use a concentration of 25 µg/mL for both extracts as this concentration was the last to generate coincident values.

Total polyphenols and flavonoids

In ▶ **Table 1**, the total content of polyphenols and flavonoids in OE and s-OE extracts are represented. From the different gallic acid concentrations, the regression equation for the polyphenol content gave 65.2 ± 3.93 mg and 66.4 ± 2.36 mg gallic acid equivalents (GAE)/g dry weight for OE and s-OE, respectively. The total flavonoid content in plant extracts was calculated as mg Rutin equivalents (RE)/g dry weight and was equal to 8.23 ± 1.31 and 7.29 ± 2.34 mg for OE and s-OE, respectively.

▶ **Table 1** Measurement of phytochemical compound concentration

Extract	Extract Polyphenols	Flavonoids
OE	65.2 ± 3.93 mg	8.23 ± 1.31 mg
s-OE	66.4 ± 2.36 mg	7.79 ± 2.34 mg

Scavenging activity

To determine the *in vitro* antioxidant effectiveness of OE and s-OE and evaluate which extract had more marked antioxidant activity, three tests were used: the DPPH (1,1-diphenyl-2-picrylhydrazyl), reducing power, and the ferrous ions chelating activity assays. The DPPH test showed that both extracts have free radical scavenging activity, which is lower than ascorbic acid but still high. After measuring the absorbance, the inhibitory concentration IC_{50} of OE and s-OE was calculated. The IC_{50} of OE was found to be 0.026 ± 0.00 029 mg/mL, while the IC_{50} of s-OE was 0.019 ± 0.0032 mg/mL (▶ **Fig. 4a**). As shown in ▶ **Fig. 4b**, OE and s-OE have a high reducing power that is slightly lower than ascorbic acid. Between the two extracts considered, s-OE showed a statistically higher effect than OE. In the Fe^{2+} chelating activity test (▶ **Fig. 4c**), OE and s-OE showed the same trend as the other assays, and s-OE showed significantly more activity at all test concentrations. In these experiments, ascorbic acid (500 µM, 24 h) was used as a positive control. In conclusion, tests used to measure the antioxidant capacity of extracts suggest that s-OE works more than OE.

Antioxidant property on cell line

After evaluating the antioxidant activity of the extracts on the powders obtained, we also studied this property on the chosen cell line. As can be seen in ▶ **Fig. 5a**, pretreatment with OE and s-OE alone did not result in any accumulation of ROS, reproducing a situation similar to that of untreated cells. In these experiments, hydrogen peroxide was used as a positive control and cells exposed to H_2O_2 (120 µM, 20′) showed an accumulation of ROS evidenced by the shift to the right of the fluorescent peak, compared to the control cells. Lead treatment caused a lower ROS production than H_2O_2 but was statistically significant. Finally, pretreatment with extracts, followed by lead exposition, reduced the accumulation of ROS, and s-OE worked better than OE, with a significant reduction. In ▶ **Fig. 5b**, the respective quantification is shown. Antioxidant properties were also assessed by measuring the malondialdehyde levels, a toxic by-product of lipid peroxidation, and the effects generated by the OE and s-OE extracts. ▶ **Fig. 5c** shows the results obtained, which have followed the same trend of ROS measurement.

The activity of primary antioxidant enzymes

When mammalian cells are subjected to oxidative stress, some antioxidant enzymes are expressed with the role of reducing and/or resolving the stressful condition and surviving. Between these, catalase (CAT), superoxide dismutase (SOD), and glutathione peroxidase (GSH-Px) are the most known. We have mea-

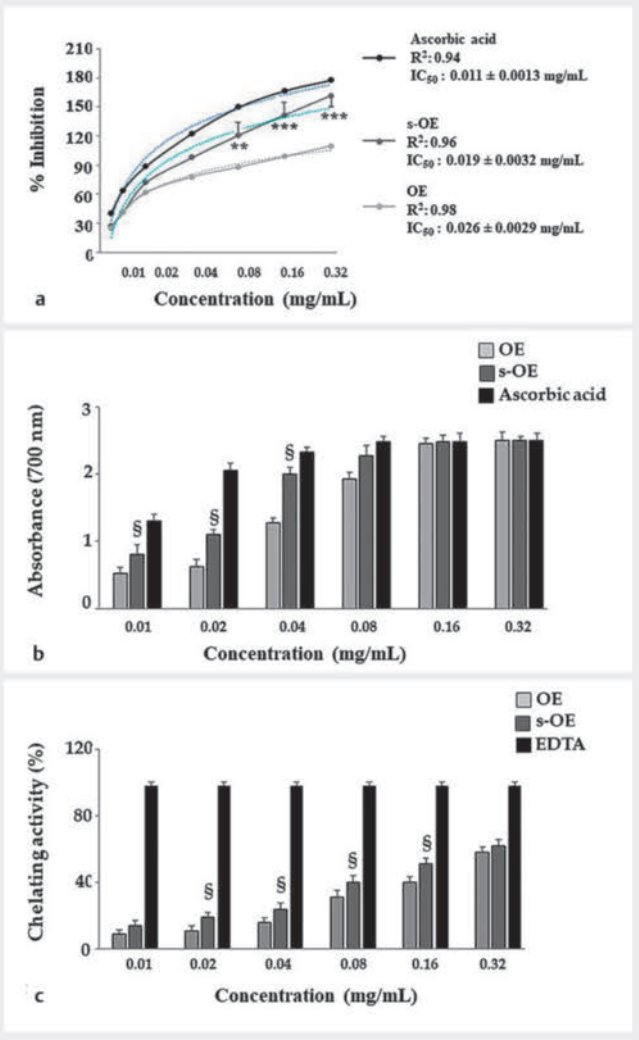

▶ **Fig. 4** Determination of OE and s-OE antioxidant activity. The DPPH, reducing power, and the ferrous ions chelating activity assays are reported in panels **a, b**, and **c**, respectively. Calculation of IC_{50} was made using GraphPad Prism software, based on the model described by Chou et al., 2005 [52]. Ascorbic acid (500 µM, 24 h) was used as positive control. Three independent experiments were carried out. ** denotes $p < 0.01$ vs. the respective value on the OE curve; *** denotes $p < 0.001$ vs. the respective value on the OE curve; § denotes $p < 0.05$ vs. OE. A Tukey–Kramer comparison test followed variance analysis (ANOVA).

sured their activity under the described test conditions. ▶ **Fig. 6** shows the results of the activities of CAT, SOD, and GSH-Px), in panels **a, b**, and **c**, respectively. As it is possible to observe, the activity of enzymes has been measured at different treatment times (0, 3, 6, 9, 12, 24, and 30 hours), and in the right part of the three panels is represented the magnification of the left panels and the statistical diversity. The results obtained by the activity of the three enzymes showed the same trend but with different orders of magnitude: the extracts alone did not alter the enzymatic activity; the treatment with lead significantly reduces it, while co-treatment improves it, compared to treatment with the lead. Again, s-OE appeared more functional than OE.

OE and s-OE protect against lead-induced damage

In ▶ **Fig. 7 a**, a significant reduction in cell viability, following exposure to increasing concentrations of lead, is represented. Treatment with the chosen concentration of lead (25 µM) resulted in a reduction in viability of about 40% compared to untreated cells. Interestingly, both extracts used have protected against lead-induced neurotoxicity, increasing cell viability. The concentration of 25 µg/mL of extract s-OE protected about 10% more than OE. In these experiments, treatment with beta-amyloid peptide (Aβ), the major constituent of amyloid plaques in Alzheimer's disease, was used as a positive control. Treatment with lead has also been associated with a reduction in lipid production, as demonstrated by appropriate cytfluorimeter readings. Specifically, lead reduced lipid levels by about 50% compared to control cells; moreover, while OE and s-OE administered alone did not alter lipid content, assuming a behavior like untreated cells, co-treatment with lead restored lipid reduction and s-OE worked significantly better than OE. This effect was shown in ▶ **Fig. 7 b**, while in ▶ **Fig. 7 c**, the respective quantification is represented.

Olea europaea extracts reduce endoplasmic reticulum stress: calcium levels and GRP-78 expression

In ▶ **Fig. 8 a**, the cytosolic level of calcium was represented, and its variations are due only to the ion coming from the endoplasmic reticulum. Treatment with thapsigargin (TAPSI), a noncompetitive Ca^{2+} ATPase sarco/endoplasmic reticulum inhibitor (SERCA), increased cellular calcium levels, forcing its release from organelle, and this effect was visible with an increase in basal calcium levels, compared to untreated cells. In ▶ **Fig. 8 b**, it was shown that treatment with OE and s-OE alone did not affect basal calcium and the respective curves overlapping those of untreated cells. The pretreatment with OE or s-OE, followed by lead exposure, reduced basal calcium levels compared to levels achieved with lead. Again, s-OE was more efficient than OE. This latter is shown in ▶ **Fig. 8 c**. Finally, the expression of GRP-78, the main chaperone of the endoplasmic reticulum, was evaluated to highlight any alterations of this organelle: as you can appreciate in ▶ **Fig. 8 d**, the treatment with lead significantly increased its expression, while pretreatment with OE and s-OE, followed by exposure to lead, reduced it, demonstrating protection from heavy metal. When the extracts of interest were tested alone, they were not responsible for altering the expression of GRP-78.

Lead treatment results in impaired cell cycle

Lead significantly altered the cell cycle profile, blocking cells in the Sub-G0 phase and reducing cell viability at the expense of the G0/G1 phase. As can be seen in ▶ **Fig. 9 a** and **b**, the Sub-G0 phase was absent in cells not treated or treated with OE and s-OE alone (3%, 2%, and 2%, respectively). In contrast, this phase increased to 61% after treatment with lead. The G0/G1 phase is reduced from about 62% (in control cells, in OE, and in s-OE) to 11% (in the lead-treated sample). Pretreatment with s-OE extract, before lead exposure, significantly restored the lead-altered cell cycle, bringing the Sub-G0 phase to 5% and the G0/G1 phase to 41%, in a condition similar to untreated or OE- and s-OE-treated cells alone. OE extract slightly improved the cell cycle profile (Sub-G0 = 38%; G0/G1= 30%) by only slightly overlapping the control cells. The quantification of the phases of the cell cycle is shown in ▶ **Fig. 9 b**.

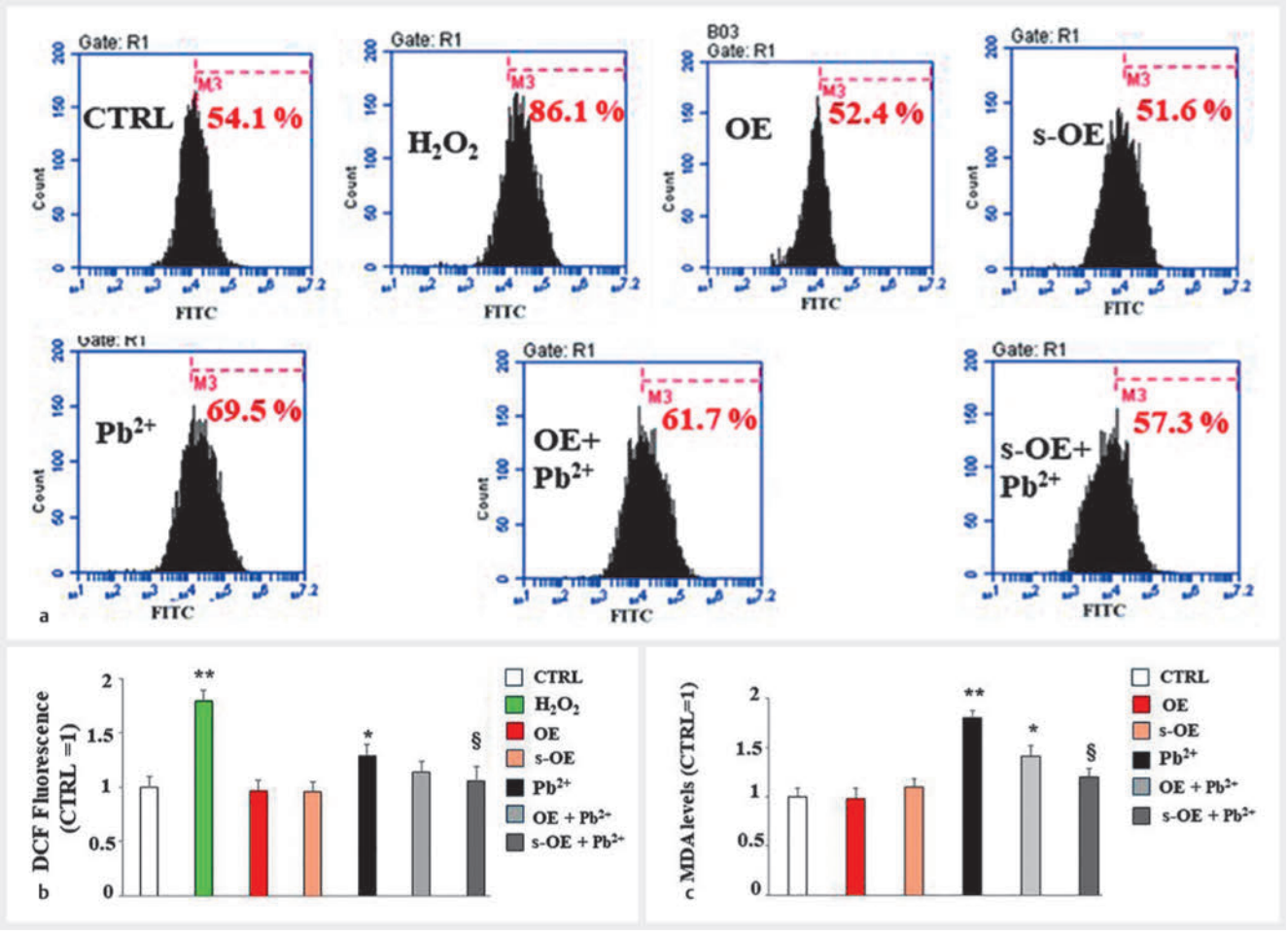

▶ **Fig. 5** ROS accumulation and malondialdehyde levels. In panel **a**, the accumulation of ROS measured with the cytofluorometer is shown. Each box refers to a treatment as indicated: the x-axis represents the fluorescence of the fluorochrome Fitc connected to our fluorescent probe, while the y-axis is relative to the number of cells that we decided to acquire (10 000). At the top of each box, there is a marker (M3), which is arbitrarily drawn in the control and kept the same for all other samples. The part of the peak included in M3 is indicated by a numerical percentage. In panel **b**, the respective quantification, obtained from comparing the percentages, is represented. The control percentage is arbitrarily made equal to 1 and the other values are related to it. Panel **c** represents the levels of malondialdehyde generated by the different treatments. Three independent experiments were carried out, and the values are expressed as the mean ± standard deviation (sd). * denotes $p < 0.05$ vs. CTRL; ** denotes $p < 0.01$ vs. CTRL; § denotes $p < 0.05$ vs. lead. Analysis of variance (ANOVA) was followed by a Tukey–Kramer comparison test.

The deleterious effects of lead are caused by oxidative damage

The smooth endoplasmic reticulum is presumably involved in the damage induced by lead exposure, as demonstrated by the alteration of lipid and calcium levels and the modulation of the GRP-78's expression. N-acetylcysteine (NAC, 2 mm for 6 hours), a known reducing agent with strong antioxidant properties, has shown an important role in adverse events generated by lead exposure. As shown in ▶ **Fig. 10**, when administered alone, NAC behaved in a similar way to untreated cells, while cell co-treatment with NAC and lead generated protection against lead-induced damage, reporting all values like untreated cells. Protection generated by NAC has been observed not only for lipid and calcium levels but also for GRP-78 expression, demonstrating a direct involvement of oxidative damage formed by lead.

Discussion and Conclusions

The first objective of this manuscript was to create an innovative extract, always obtained from olive leaves like OE but subject to a sonication process (s-OE). It has been reported that the use of sonication could intensify the dissolution process, increasing the solubility and water dispersion rate of the sonicate compound [33]. Ultrasonic homogenization involves a wide variety of effects, and its action depends on sonication conditions, especially sonication time and sonication power [34]. The increased solubility of s-OE after sonication can be explained by several factors such as changes in particle size, morphology, and degree of crystallinity [35]. During the sonication process, the extract was always kept in a container containing ice to prevent its overheating, with hypothetical breakage of its chemical components, and because it has been shown that the combination of sonication in an ice bath

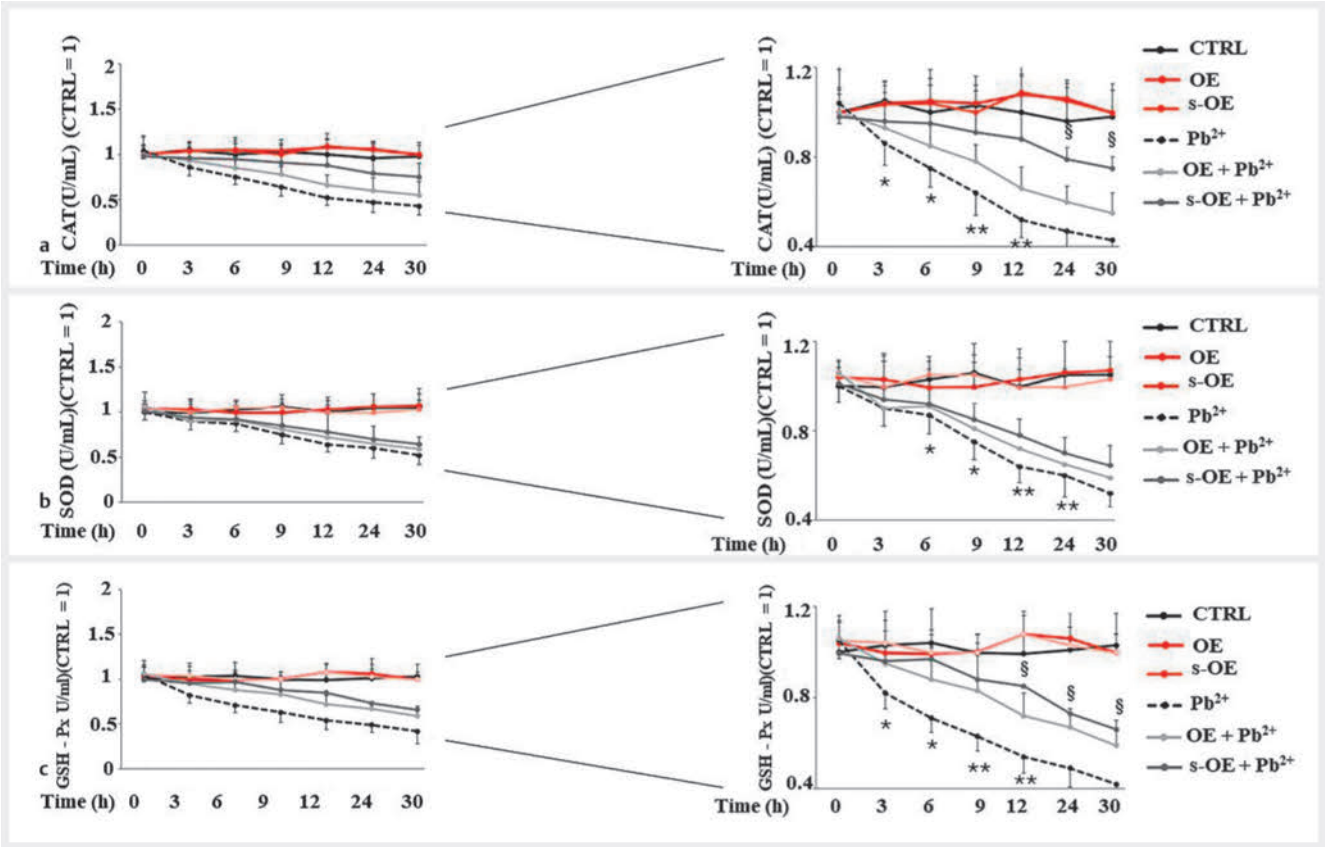

▶ **Fig. 6** CAT, SOD, and GSH-Px activities. The activities of these enzymes are represented in panels **a, b**, and **c** respectively. The left part of the panels shows the values of the activities, while the right part shows the magnification of the left part and the statistical analysis. The enzymatic activity was followed at different times (3, 6, 9, 12, 24 and 30 h). Three independent experiments were carried out, and the values were expressed as the mean ± standard deviation (sd). * denotes $p < 0.05$ vs. the time 0; * * denotes $p < 0.01$ vs. the time 0; § denotes $p < 0.05$ vs. OE + Pb^{2+}. Analysis of variance (ANOVA) was followed by a Tukey–Kramer comparison test.

increases the efficiency of solubility [36]. In addition, the sonication process has also made it possible to reduce the amount of EtOH used, passing from a hydro-alcoholic solution (EtOH: H_2O = 70 : 30) to another (EtOH: H_2O = 50 : 50). A reduced amount of EtOH makes s-OE safer and more sustainable [37]. As prolonged exposure to ethanol causes numerous health-damaging effects [38], the reduction in this alcohol in the preparation of s-OE contributes to the achievement of environmental sustainability [39]. Finally, it should also be noted that the extract s-OE is more effective than OE in the protection from neurotoxicity induced by lead exposure. Presumably, the best dissolution of the extract has enhanced its functionality. Most of the literature shows that lead exposure causes oxidative damage accompanied by mitochondrial alteration, imbalance of the oxidant-antioxidant system, cytochrome c leakage, and apoptosis [40, 41]. In our experimental model, we appreciated oxidative damage caused by exposure to lead, as demonstrated by an accumulation of ROS, an increase in the levels of malondialdehyde, and an alteration of the levels of activity of the main antioxidant enzymes. Moreover, our experimental work has also shown that the neurotoxicity induced by exposure to lead involves the dysfunction of the cellular organelle endoplasmic reticulum: an alteration of the calcium preserved in this organelle and the reduction in lipid synthesis, two aspects governed generally by the smooth endoplasmic reticulum [42]. The involvement of the endoplasmic reticulum has been also confirmed by the modulation of the expression of GRP78, a chaperone that plays a key role in the control of cellular stress, in the folding of proteins, in the degradation of unfolded proteins, and in endoplasmic reticulum lumen quality control [43]. A consequence of lead exposure and calcium leakage from the endoplasmic reticulum is also an impaired distribution of cell cycle phases [44] with a significant increase in cell death in the Sub-G0 phase. This assumption could be justified by a dysregulation of the cell cycle, dependent on cellular calcium [45]. However, the mechanism involving the endoplasmic reticulum results as a consequence of the oxidative damage generated by lead. We hypothesize that lead exposure determines the production and accumulation of reactive species, responsible for an alteration of the endoplasmic reticulum, altering the physiological cross-talk between mitochondria and endoplasmic reticulum [46]. This hypothesis seems to be confirmed by the results obtained with the pretreatment with the antioxidant N-acetylcysteine, which has restored almost completely all lead-induced dysfunctions, reverting lipid and calcium ion reduction as well as avoiding endoplasmic reticu-

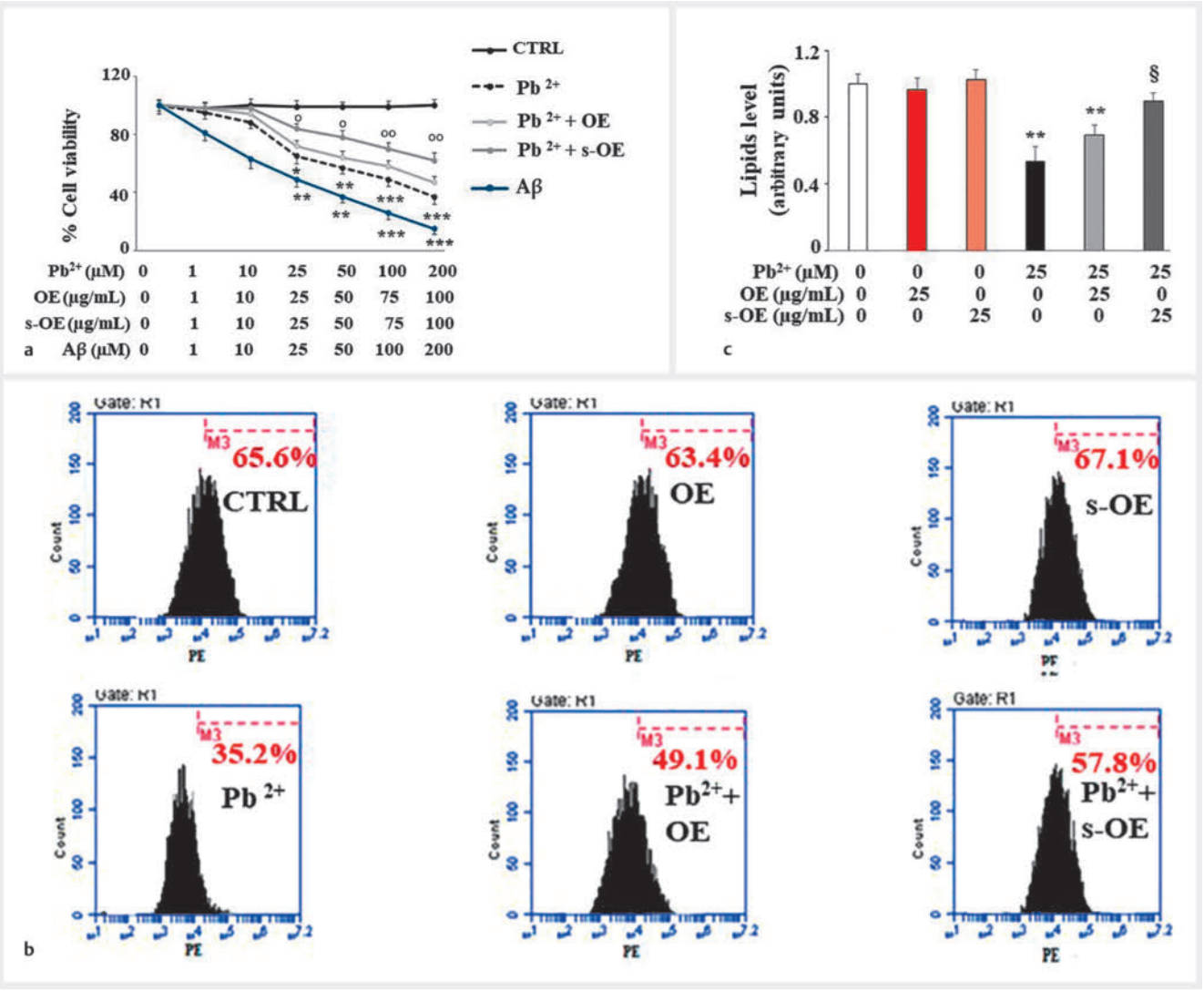

▶ **Fig. 7** The treatment with lead has induced cellular damage: viability and lipid decrease. Panel **a** shows the significant reduction in viability following exposure to increasing concentrations of lead. The concentration chosen was 25 μM, which was able to determine a reduction in viability of 40% compared to untreated cells. Treatment with A*β* was used as a positive control. In panel **b**, a cytofluorometric reading is represented that highlights the reduction in lipid synthesis induced by lead exposure. In particular, the lipid reduction has been evidenced by the shift on the left of the fluorescent cellular peak, compared to untreated cells. In every single box of panel **b**, the x-axis represents the fluorescence of fluorochrome PE linked to our fluorescent probe, while the y-axis is relative to the number of cells that we have decided to acquire (20 000). At the top of each box, there is a marker (M3), which is arbitrarily drawn in the control and kept the same for all other samples. The part of the peak included in M3 is indicated by a numerical percentage. In panel **c**, the respective quantification, obtained from comparing the percentages, is represented. The control percentage is arbitrarily made equal to 1, and the other values are related to it. Three independent experiments were performed, and the values were expressed as the mean ± sd. * denotes $p < 0.05$ vs. the control; ** denotes $p < 0.01$ vs. the control; *** denotes $p < 0.001$ vs. the control. ° denotes $p < 0.05$ vs. the corresponding concentration of OE + Pb^{2+}; °° denotes $p < 0.01$ vs. the corresponding concentration of OE + Pb^{2+}; § denotes $p < 0.05$ vs. Pb^{2+}. Variance analysis (ANOVA) was followed by a Tukey–Kramer comparison test.

lum involvement, as demonstrated by GRP-78 expression after NAC-lead co-treatment. Since pretreatment with OE and s-OE can significantly reduce the damage caused by lead (s-OE OE), they are expected to have an antioxidant effect. The antioxidant activity of the extracts could be justified both by the presence of total polyphenols-flavonoids and by the high concentration of oleuropein and hydroxytyrosol present in the extracts. All these compounds are particularly known for their protective role in oxidative damage [47]. The results obtained are interesting and promising, but they belong to a preliminary study conducted *in vitro* (on OE and s-OE extracts and a cell line). This research has led us for the first time to the knowledge of s-OE and the use of both extracts in protection from harmful lead exposure. However, further research is needed to confirm these effects *in vivo* under conditions that include all physiological processes. For example, it would be desirable to conduct investigations on the bioavailability of these extracts even after ingestion, digestion, and expulsion [48, 49]. The concentration of extracts used in this work (25 μM)

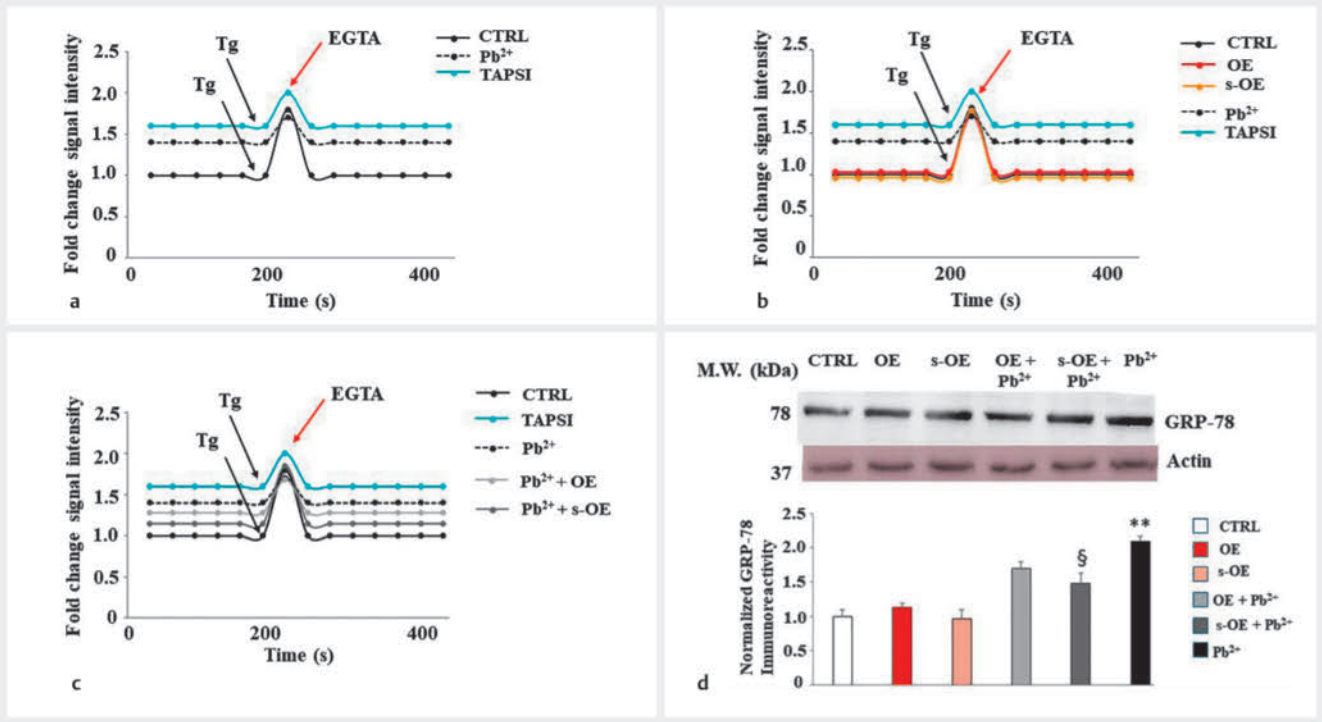

▶ **Fig. 8** Measurement of cytosolic calcium. Untreated cells consist of a specific level of calcium ions, which is expected to increase because of TAPSI exposure, as indicated by the black arrow. Subsequently, treatment with EGTA, a chelating agent, reduces calcium levels, as represented by the red arrow. Exposure to lead increased the basal calcium levels compared to untreated cells. Panel **a** represents an experimental model that testifies to the operation of this method. Panel **b** highlights the calcium levels generated by treatment with OE and s-OE alone and compares them to those generated by TAPSI and Pb^{2+}. In panel **c**, calcium levels after pretreatment with OE/s–OE and lead exposure are shown. The figure reports a representative experiment. Panel **d** shows the modulation of the expression of GRP-78 in our experimental model, normalized for the housekeeping protein actin. The respective quantification is highlighted under Western blotting. Three independent experiments were performed, and the values were expressed as the mean ± sd. ** denotes $p < 0.01$ vs. the control; § denotes $p < 0.05$ vs. lead. A representative image is shown. Analysis of variance (ANOVA) was followed by the Tukey–Kramer comparison test.

was chosen because it was safe and non-toxic in the models considered. Although in studies *in vivo* the concentration of extracts used will be higher than that represented in this manuscript, this research will have been useful in highlighting the mechanisms involved in protecting the extracts against lead. If the results obtained are confirmed also *in vivo*, the use of *Olea europea* could increase considerably, and this plant could guarantee further specific remedies for human health. In conclusion, we can say that:

1. Sonicated extract (s-OE) works better than OE. Therefore, the use of sonication is promising and could justify further research to understand if the increased solubility and dissolution rate can also affect the bioavailability of the extract *in vivo*.
2. Lead exposure causes damage to the mitochondria-reticulum endoplasmic unit in human neurons, which can be attributed to oxidative damage.

Materials and Methods

Plant materials and sample preparation

The leaves of the olive tree (*Olea europaea*, cultivar Coratina) were collected in Roccelletta di Borgia, Calabria, Italy, latitude 20°25′ 47′′N and longitude 34°27′36′′E (February 2023, temperature 9,2 °C). The taxonomic identification was confirmed by full professor Salvatore Ragusa, University "Magna Graecia" of Catanzaro (author of this manuscript). The voucher specimen was deposited in the Department of Health Sciences, University "Magna Graecia" of Catanzaro under the following accession number *Olea Europaea* L., cv. Coratina: 12. Several washes with MilliQ water were carried out to remove pollution or other contaminants from leaves. Then, 100 g of dried and milled leaves and 800 mL of water were placed in a Pyrex round-bottomed flask equipped with a jacketed coiled condenser in a domestic microwave oven [31]. After extraction, performed by irradiation at 800 W for 10 min, leaves were filtered, and the obtained solution was dried under pressure. To eliminate the solid residue, the extract was filtered with acetone, and the solution was evaporated under pressure to obtain the crude extract (OE). Subsequently, the OE was placed in dark bottles and stored at 4 °C before being used. To carry out the experiments, the OE was dissolved in a hydroalcoholic solution composed of EtOH : water (70 : 30).

s-OE preparation

s-OE was obtained by dissolving the OE powder in a hydroalcoholic solution in which the ratio of EtOH to water was 50 : 50 and then subjected to a sonication treatment (frequency of 15 kHz,

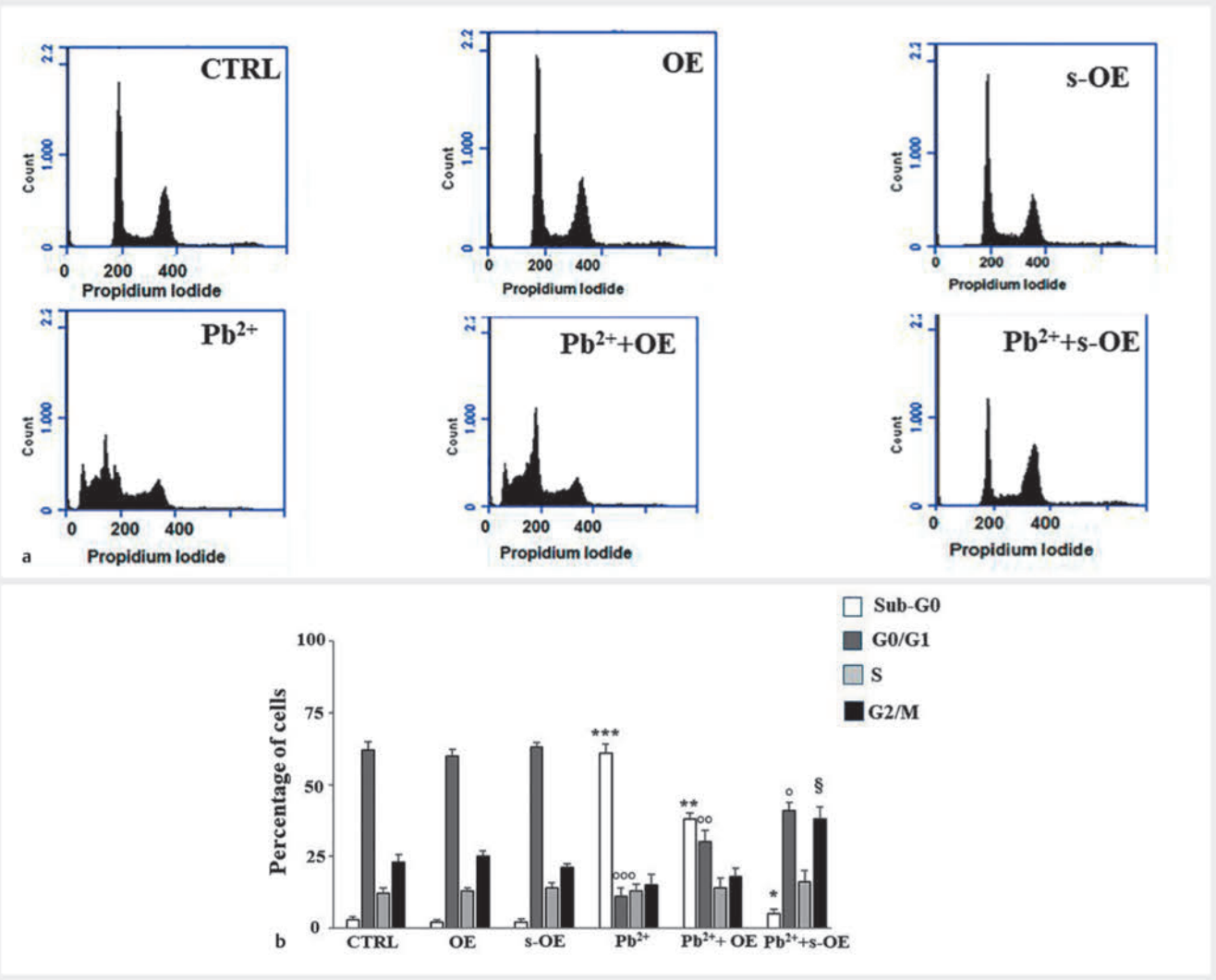

▶ **Fig. 9** Exposure to lead alters the cell cycle profile. This figure shows the cell cycle obtained by cytofluorometric analysis. In every single box of panel **a**, the x-axis represents the fluorescence of the propidium iodide, while the y-axis is relative to the number of cells that we have decided to acquire (30 000). In panel **b**, the respective quantification is shown. Three independent experiments were performed, and the values were expressed as the mean ± sd. * denotes $p < 0.05$ vs. Sub-G0 phase of the control; ** denotes $p < 0.01$ vs. Sub-G0 phase of the control; *** denotes $p < 0.001$ vs. Sub-G0 phase of the control. ° denotes $p < 0.05$ vs. G0/G1 phase of the control; °° denotes $p < 0.01$ vs. G0/G1 phase of the control; °°° denotes $p < 0.001$ vs. G0/G1 phase of the control. § denotes $p < 0.05$ vs. G2/M phase of the control. Variance analysis (ANOVA) was followed by a Tukey–Kramer comparison test.

power 470 W for 10 min, Bandelin electronic) under constant stirring (150 rpm). s-OE was always kept in a container containing ice. s-OE was placed in dark bottles and stored at 4 °C before being used for experimentation. The choice of power to be used was justified by previous experiments in our laboratory.

UHPLC-UV-ESI-HRMS analysis

The quantification of hydroxytyrosol and oleuropein in Coratina leaves dry extract was performed by reverse-phase ultra-high-performance liquid chromatography followed by electrospray high-resolution mass spectrometry, with ionization in negative mode, as reported by Frisina et al. [32]. Chromatography separation was performed using a Dionex Ultimate 3000 RS (Thermo Scientific), equipped with a Hypersil Gold C18 column (100 × 2.1 mm, 1.9 µm particle size, Thermo Scientific), which was thermostated at 24 °C. The chromatographic column was equilibrated in 98% solvent A (ultrapure water containing 0.1% of formic acid) and 2% solvent B (methanol). The flow rate on the column was maintained at 300 µl · min^{-1} and the concentration of solvent B was linearly increased from 2% to 23% in 6 min, remaining in isocratic for 5 min, then linearly increased from 23% to 50% in 7 min and from 50% to 98% in 5 min, remaining in isocratic for 6 min, and finally returned to 2% in 6 min, remaining in isocratic for 3 min. The UV/VIS detector was set at 235, 254, 280, and 330 nm. Mass detection was performed by a high-resolution Q-Exactive orbitrap mass spectrometer (Thermo Scientific). In each scan, the negative exact mass $[M - H]^-$ of hydroxytyrosol (153.0557 m/z) and oleuropein precursors (539.1170 m/z) were selected in parallel reaction

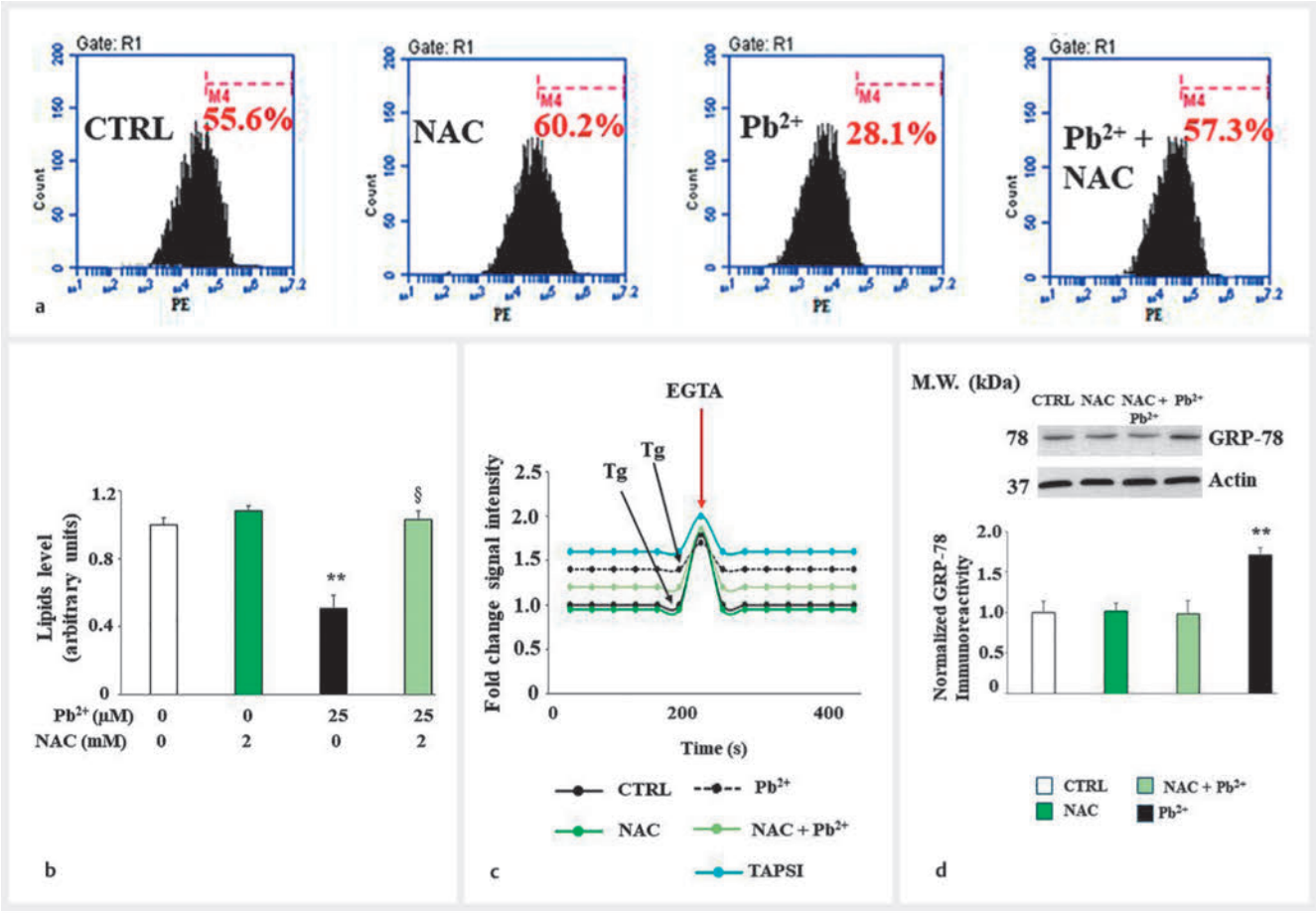

▶ **Fig. 10** Effects of NAC on lead-induced damage. Panel **a** showed the effect of NAC on the lead-induced reduction in lipid levels, while panel **b** highlighted the respective quantification. Calcium ion levels after treatment with NAC are represented in panel **c**. Finally, panel **d** reported the expression of the protein GRP-78 after co-treatment with NAC–lead. Values of three independent experiments are indicated, and a representative image is shown. ** denotes $p < 0.01$ vs. CTRL; § denotes $p < 0.05$ vs. lead. Analysis of variance (ANOVA) was followed by the Tukey–Kramer comparison test.

monitoring. Hydroxytyrosol and oleuropein were characterized according to the corresponding HRMS spectra, accurate masses, characteristic fragmentations, and retention times. Xcalibur software (version 4.1) was used for instrument control, data acquisition, and data analysis.

Measurement of polyphenols content

The total polyphenols were quantified by the Folin–Ciocalteu assay using gallic acid 99% (Sigma-Aldrich) as the reference standard. The extracts OE or s-OE were prepared by adding 20 mL of ethanol/water 50:50 (w/w) to 1 g of powder to obtain absorbance values within the linearity range of the calibration curve. The mixture obtained was stirred for 24 h at 20 °C. Then, 400 µL of extract was added to 0.8 mL of Folin–Ciocalteu reagent diluted 10 times. After 3 minutes, 0.8 mL of sodium carbonate 7% (w/v) was added, and the mixture was allowed to stand for 2 h with constant stirring. The absorbance was measured at 760 nm with a Prism V-1200 spectrophotometer. The total phenolic content was determined from the linear equation of a standard curve prepared with different concentrations of gallic acid, and the results were expressed in mg of gallic acid equivalents per g of dry weight.

Measurement of flavonoid content

The flavonoid content of the extracts was measured by the colorimetric technique of aluminum chloride. Specifically, 1 mL of extract was mixed with 1 mL of 2% aluminum chloride in methanol. After 30 min, the absorbance at 510 nm was measured, and the rutin equivalents (mg RE/g extract) were used to represent the estimated content of flavonoids.

Free radical scavenging activity

The free radical scavenging activity of both extracts was determined using the stable radical 2,20 -diphenyl-1 picrylhydrazyl (DPPH) in which samples were tested at different concentrations (0.01–0.32 mg/mL) [50]. Experimentally, an aliquot (0.5 mL) of samples was added to 3 mL of DPPH solution, keeping the mixture in the dark for 20 min. Subsequently, the absorbance was read by a UV-Vis spectrophotometer (Multiskan GO, Thermo Scientific) at 517 nm and at room temperature. Ascorbic acid was used as a reference. The results are reported as an average percentage of radical scavenging activity (%) and were expressed also as % inhibition value and IC_{50}.

Reducing power assay

This method is based on the principle that substances with a reducing potential react with potassium ferricyanide (Fe^{3+}) to form potassium ferrocyanide (Fe^{2+}). The reducing power of OE and s-OE extracts has been evaluated by spectrophotometric detection of the Fe^{3+}-Fe^{2+} transformation method [51]. The samples were tested at different concentrations (0.01–0.32 mg/mL); different amounts of samples in 1 mL solvent were mixed with 2.5 mL phosphate buffer (0.2 M, pH 6.6) and 2.5 mL potassium ferricyanide at 1% [K3Fe(CN)6]. The mixture was incubated at 50 °C for 20 min. The solution was quickly cooled, mixed with 2.5 mL of 10% trichloroacetic acid, and centrifuged at 1811 rcf for 10 min. The resulting supernatant was mixed with 2.5 mL of distilled water and 0.5 mL of 0.1% fresh ferric chloride ($FeCl_3$), and the absorbance was measured at 700 nm after 10 min. Ascorbic acid was used as a reference. The reducing potential was expressed in ascorbic acid equivalent (ASE/mL).

Ferrous ions (Fe^{2+}) chelating activity

The Fe^{2+} ions have pro-oxidant properties capable of determining lipid oxidation resulting in cellular alterations, and chelating agents can reduce these damages. The chelating activity can be studied by spectrophotometric evaluation of the inhibition of the Fe^{2+}-ferrozine complex in which the agents reduce the formation of this complex: the reduction in the color is proportional to the chelating activity produced. Experimentally different concentrations of each sample in 1 mL solvent were mixed with 0.5 mL methanol and 0.05 mL of 2 mM $FeCl_2$. The mixture obtained was vigorously mixed and maintained at room temperature for 10 min. The absorbance of the solution was measured spectrophotometrically at 562 nm.

Cell cultures

A cell line of human neurons (SH-SY5Y) was acquired from the American Type Culture Collection and kept in Eagle's minimum essential medium supplemented with nonessential amino acids, 10% fetal bovine serum, penicillin (100 IU/mL), and streptomycin (100 µg/mL). The cell line was cultivated in a 5% humidified CO_2 atmosphere at 37 °C. To differentiate SH-SY5Y cells, 10 µM of all-trans-retinoic acid was used for 5 days. When the cells reached 60% confluence, they were treated with OE or s-OE 25 µg/mL for 24 h. In neurotoxicity-induced studies, the cells were pretreated with OE or s-OE and then exposed to Pb^{2+} for an additional 24 h. Finally, in experiments conducted to study the antioxidant effect of NAC, the cells were treated with NAC, 2 mM, for 6 hours and successively exposed to Pb^{2+} for an additional 24 h.

Measurement of cell viability through MTT test

3-(4,5-dimethylthiazol-2-yl)-2,5-diphenyltetrazolium bromide (MTT) was used to evaluate cell viability in a colorimetric assay. Then, 8×10^3 cells were grown in 96-well plates, and the treatments were performed as indicated. The medium was replaced with a phenol-free medium containing an MTT solution (0.5 mg/mL). Finally, after 4 h incubation, 100 µL of 10% SDS was added to solubilize formazan crystals, and the optical density was measured at wavelengths of 540 and 690 nm using a spectrophotometric reader (X MARK Microplate Bio-Rad).

Measurement of ROS accumulation in cells

The molecule H_2 DCF-DA easily enters cells and is subsequently cleaved by intracellular esterases to form H_2 DCF, which is not more able to leave cells and, if oxidized, binds to ROS, forming the compound DCF highly fluorescent. Therefore, the quantification of the DCF probe provides the content of ROS in cells. Experimentally, SH-SY5Y cells were seeded in 96-well microplates with a density of 6×10^4. The following day, they were pretreated with OE and s-OE at a concentration of 25 mg/mL for 24 hours. At the end of the treatment, the growth medium was replaced with a fresh medium containing H_2DCF-DA (25 µM), and after 30 minutes of exposure to 37 °C, the cells were washed with PBS, centrifuged, resuspended in PBS, and exposed or not to H_2O_2 (120 µM, 20 min). Fluorescence was evaluated by cytometric analysis (FACS Accury, Becton Dickinson).

Catalase, superoxide dismutase, and glutathione peroxidase activities

Following the treatments carried out as described, the activities of CAT, SOD, and GSH-Px were measured in SH-SY5Y cells. For this purpose, the respective kits (UK, Cambridge, and Abcam) were used according to the manufacturers' instructions. The CAT enzyme converts hydrogen peroxide into another compound that can be measured at 570 nanometers, whose activity is inversely proportional to the measured signal. The SOD enzyme converts superoxide radicals into hydrogen peroxide and molecular oxygen. When measuring its activity, superoxide anions react with a specific probe to produce a water-soluble formazanic dye. The higher the activity of SOD in the sample, the lower the production of dye formazan. Finally, GSH-Px converts hydrogen peroxide into water in a reaction involving glutathione and determines the consumption of NADPH. NADPH reduction is measured at 340 nanometers and is proportional to Gpx activity.

Lipid quantification by flow cytometry

Nile red (excitation/emission ~ 552/636) is a dye that binds tightly to cellular lipids. At the end of the appropriate treatments, the neurons were collected and adequately incubated with 1 µg/mL of Nile red dye for 15 min in the dark and protected from light. Subsequently, the cells were washed in PBS (pH = 7.4) and immediately read in the flow cytometer FACS Accury (Becton Dickinson).

Cell lysis and immunoblot analysis

The cells SH-SY5Y, grown in 100 mm plates, were washed with PBS and lysed with a preheated lysis buffer containing 50 mM TrisCl, pH 6.8, 2% SDS, and a mixture of protease inhibitors. The protein concentration in cell lysates was determined from the DCA protein assay; the samples were boiled and filled with SDS-polyacrylamide gel (10%). After electrophoresis, polypeptides were transferred, and specific antibodies were used to reveal the respective antigens. The primary antibodies were incubated overnight at 4 °C followed by a secondary antibody conjugated with horseradish peroxidase for 1 hour at room temperature. The blots have been developed by advanced chemiluminescence procedures. The following primary antibodies were used: a monoclonal antibody for GRP-78 made in the rabbit (ab21685, abcam) at 1 : 1000 dilution and a monoclonal anti-actin antibody made in

the mouse at dilution 1 : 5000. Secondary antibodies conjugated with horseradish peroxidases made in rabbit or mouse were used at 1 : 10 000 dilution.

Intracellular calcium measurements

The rhodamine 2 fluorescent probe is frequently used to measure the intracellular calcium since it binds to this ion. The neurons, after being treated as indicated, were exposed to Rhod 2 for 1 h at 25 °C and protected from light. At the end of the exposure time, they were washed in a calcium- and magnesium-free solution to prevent the entering of calcium from the extracellular environment and subjected to flow cytometric analysis. The cells were also treated with a decoupling of mitochondrial oxidative phosphorylation, carbonylcianuro-4-(trifluoromethoxy) phenylhydrazone (FCCP, 1 µM), and oligomycin (1 µg/mL), a mitochondrial ATPase inhibitor. Both treatments may exclude mitochondrial calcium involvement. Thus, any movement of calcium was related to endoplasmic reticulum calcium. A cytofluorometer reading (Accury, Becton Dickinson) provides the basal concentration of the calcium ion in cells.

Cell cycle analysis

The cell cycle refers to the events through which a cell grows, replicates its genome, and eventually divides into two daughter cells through the process of mitosis. Briefly, SH-SY5Y cells were seeded in 100 mm plates. After the treatments carried out as described, the cells were collected, washed twice with PBS, and fixed in 70 % cold ethanol for at least 2 hours at 20 °C. After fixation, the cells were washed with PBS and incubated with 1 mL PBS containing 0.5 mg/mL RNAse A and 0.5 % Triton X-100 for 30 minutes at 37 °C. Finally, the cells were stained with 50 mg/mL of propidium iodide and analyzed by flow cytometry using a FACS Canto II system (BD Biosciences). The various phases of the cell cycle were determined using FACS Diva software v. 6.1.3 (BD Biosciences).

Contributors' Statement

J. M., S. B., and G. D. have conceptualized and designed the manuscript; J. M., F. B., S. R. have collected and produced data; J. M. and L. G. have interpreted data; J. M., and A. L. dealt with the statistical analysis; A. L., R. C., E. P., V. M., and S. R. have participated in the original draft preparation and curated the manuscript; J. M. and G. D. have written, revised, and supervised the manuscript.

Funding Information

Work supported by #NEXTGENERATIONEU (NGEU) and fund. by the Ministry of Univ. and Research (MUR), Nat. Recov. and Resil. Plan (NRRP), project MNESYS (PE0000006) – a multisc. integr. approach to the study of the nervous system in health and disease (DN. 1553 11. 10. 2022),and the European Commission's FESR FSE 2014–2020 and POR CALABRIA FESR AZIONE 1.5.1 "Support for research infrastructures considered critical/crucial for regional systems" Nuova Piattaforma di Farmacologia Integrata e Tecnologie Avanzate.

Conflict of Interest

The authors declare that they have no conflict of interest. The corresponding author declares that the manuscript was read, accepted, and submitted by all authors.

References

[1] Cutuli D, Petrosini L, Gelfo F. Advance in neurotoxicity research from development to aging. Int J Mol Sci 2023; 24: 15112

[2] Lamoreaux J. "Passing Down Pollution": (Inter)generational toxicology and (epi)genetic environmental health. Med Anthropol Q 2021; 35: 529–546

[3] Sayre LM, Perry G, Atwood CS, Smith MA. The role of metals in neurodegenerative diseases. Cell Mol Biol (Noisy-le-grand) 2000; 46: 731–741

[4] Al Osman M, Yang F, Massey IY. Exposure routes and health effects of heavy metals on children. Biometals 2019; 32: 563–573

[5] Babić Leko M, Mihelčić M, Jurasović J, Nikolac Perković M, Španić E, Sekovanić A, Orct T, Zubčić K, Langer Horvat L, Pleić N, Kiđemet-Piskač S, Vogrinc Ž, Pivac N, Diana A, Borovečki F, Hof PR, Šimić G. Heavy metals and essential metals are associated with cerebrospinal fluid biomarkers of alzheimer's disease. Int J Mol Sci 2022; 24: 467

[6] Vellingiri B, Suriyanarayanan A, Abraham KS, Venkatesan D, Iyer M, Raj N, Gopalakrishnan AV. Influence of heavy metals in Parkinson's disease: An overview. J Neurol 2022; 269: 5798–5811

[7] Sarihi S, Niknam M, Mahjour S, Hosseini-Bensenjan M, Moazzen F, Soltanabadi S, Akbari H. Toxic heavy metal concentrations in multiple sclerosis patients: A systematic review and meta-analysis. EXCLI J 2021; 20: 1571–1584

[8] Farace C, Fenu G, Lintas S, Oggiano R, Pisano A, Sabalic A, Solinas G, Bocca B, Forte G, Madeddu R. Amyotrophic lateral sclerosis and lead: A systematic update. Neurotoxicology 2020; 81: 80–88

[9] de Paula Arrifano G, Crespo-Lopez ME, Lopes-Araújo A, Santos-Sacramento L, Barthelemy JL, de Nazaré CGL, Freitas LGR, Augusto-Oliveira M. Neurotoxicity and the global worst pollutants: Astroglial Involvement in arsenic, lead, and mercury intoxication. Neurochem Res 2023; 48: 1047–1065

[10] Ravipati ES, Mahajan NN, Sharma S, Hatware KV, Patil K. The toxicological effects of lead and its analytical trends: An update from 2000 to 2018. Crit Rev Anal Chem 2021; 51: 87–102

[11] Patrick L. Lead toxicity part II: The role of free radical damage and the use of antioxidants in the pathology and treatment of lead toxicity. Altern Med Rev 2006; 11: 114–127

[12] Hornedo-Ortega R, Cerezo AB, de Pablos RM, Krisa S, Richard T, García-Parrilla MC, Troncoso AM. Phenolic compounds characteristic of the mediterranean diet in mitigating microglia-mediated neuroinflammation. Front Cell Neurosci 2018; 12: 373

[13] Bucciantini M, Leri M, Nardiello P, Casamenti F, Stefani M. Olive polyphenols: Antioxidant and anti-inflammatory properties. Antioxidants (Basel) 2021; 10: 1044

[14] Vazquez-Aguilar A, Sanchez-Rodriguez E, Rodriguez-Perez C, Rangel-Huerta OD, Mesa MD. Metabolomic-based studies of the intake of virgin olive oil: A comprehensive review. Metabolites 2023; 13: 472

[15] Rodríguez-Juan E, Rodríguez-Romero C, Fernández-Bolaños J, Florido MC, Garcia-Borrego A. Phenolic compounds from virgin olive oil obtained by natural deep eutectic solvent (NADES): Effect of the extraction and recovery conditions. J Food Sci Technol 2021; 58: 552–561

[16] Silvestrini A, Giordani C, Bonacci S, Giuliani A, Ramini D, Matacchione G, Sabbatinelli J, Di Valerio S, Pacetti D, Procopio AD, Procopio A, Rippo MR. Anti-Inflammatory effects of olive leaf extract and its bioactive compounds oleacin and oleuropein-aglycone on senescent endothelial and small airway epithelial cells. Antioxidants (Basel) 2023; 12: 1509

[17] Cirmi S, Celano M, Lombardo GE, Maggisano V, Procopio A, Russo D, Navarra M. Oleacein inhibits STAT3, activates the apoptotic machinery, and exerts anti-metastatic effects in the SH-SY5Y human neuroblastoma cells. Food Funct 2020; 11: 3271–3279

[18] Cirmi S, Maugeri A, Russo C, Musumeci L, Navarra M, Lombardo GE. Oleacein attenuates lipopolysaccharide-induced inflammation in THP-1-de-

rived macrophages by the inhibition of TLR4/MyD88/NF-kappaB pathway. Int J Mol Sci 2022; 23: 1206

[19] Aydin C, Ozcan MM, Gümüş T. Nutritional and technological characteristics of olive (Olea europea L.) fruit and oil: Two varieties growing in two different locations of Turkey. Int J Food Sci Nutr 2009; 60: 365–373

[20] Azbar N, Keskin T, Yuruyen A. Enhancement of biogas production from olive mill effluent (OME) by co-digestion. Biomass Bioen 2008; 32: 1195–1201

[21] Nunes LJR, Loureiro LME, Sa LCR, Silva HFC. Evaluation of the potential for energy recovery from olive oil industry waste: Thermochemical conversion technologies as fuel improvement methods. Fuel (Lond) 2020; 279: 118536

[22] Wang W, Scali M, Vignani R, Spadafora A, Sensi E, Mazzuca S, Cresti M. Protein extraction for two-dimensional electrophoresis from olive leaf, a plant tissue containing high levels of interfering compounds. Electrophoresis 2003; 24: 2369–2375

[23] Gómez-González S, Ruiz-Jiménez J, Priego-Capote F, Luque de Castro MD. Qualitative and quantitative sugar profiling in olive fruits, leaves, and stems by gas chromatography-tandem mass spectrometry (GC-MS/MS) after ultrasound-assisted leaching. J Agric Food Chem 2010; 58: 12292–12299

[24] Jaber H, Ayadi M, Makni J, Rigane G, Sayadi S, Bouaziz M. Stabilization of refined olive oil by enrichment with chlorophyll pigments extracted from Chemlali olive leaves. Eur J Lipid Sci Technol 2012; 114: 1274–1283

[25] Talhaoui N, Taamalli A, Gomez-Caravaca AM, Fernandez-Gutierrez A, Segura-Carretero A. Phenolic compounds in olive leaves: Analytical determination, biotic and abiotic influence, and health benefits. Food Res Int 2015; 77: 92–108

[26] Romani A, Ieri F, Urciuoli S, Noce A, Marrone G, Nediani C, Bernini R. Health effects of phenolic compounds found in extra-virgin olive oil, by-products, and leaf of olea europaea L. Nutrients 2019; 11: 1776

[27] Lama-Muñoz A, Del Mar Contreras M, Espínola F, Moya M, de Torres A, Romero I, Castro E. Extraction of oleuropein and luteolin-7-O-glucoside from olive leaves: Optimization of technique and operating conditions. Food Chem 2019; 293: 161–168

[28] Selim S, Albqmi M, Al-Sanea MM, Alnusaire TS, Almuhayawi MS, Hussein S, Warrad M, El-Saadony MT. Valorizing the usage of olive leaves, bioactive compounds, biological activities, and food applications: A comprehensive review. Front Nutr 2022; 9: 1008349

[29] Sahin S, Bilgin M. Olive tree (Olea europaea L.) leaf as a waste by-product of table olive and olive oil industry: A review. J Sci Food Agric 2018; 98: 1271–1279

[30] Mohapatra D, Agrawal AK, Sahu AN. Exploring the potential of solid dispersion for improving solubility, dissolution & bioavailability of herbal extracts, enriched fractions, and bioactives. J Microencapsul 2021; 38: 594–612

[31] Procopio A, Alcaro S, Nardi M, Oliverio M, Ortuso F, Sacchetta P, Pieragostino D, Sindona G. Synthesis, biological evaluation, and molecular modeling of oleuropein and its semisynthetic derivatives as cyclooxygenase inhibitors. J Agric Food Chem 2009; 57: 11161–11167

[32] Frisina M, Bonacci S, Oliverio M, Nardi M, Vatrano TP, Procopio A. Storage effects on bioactive phenols in calabrian monovarietal extra virgin olive oils based on the efsa health claim. Foods 2023; 12: 3799

[33] Li T, Wu W, Zhang J, Wu Q, Zhu S, Niu E, Wang S, Jiang C, Liu D, Zhang C. Antioxidant capacity of free and bound phenolics from olive leaves: In vitro and in vivo responses. Antioxidants (Basel) 2023; 12: 2033

[34] Pereira SV, Colombo FB, de Freitas LAP. Ultrasound influence on the solubility of solid dispersions prepared for a poorly soluble drug. Ultrason Sonochem 2016; 29: 461–469

[35] Kumar TS, Shanmugam S, Palvannan T, Kumar VMB. Evaluation of antioxidant properties of Elaeocarpus ganitrus Roxb. 615 leaves. Iran J Pharm Res 2008; 7: 211–215

[36] Sandilya DK, Kannan A. Effect of ultrasound on the solubility limit of a sparingly soluble solid. Ultrason Sonochem 2010; 17: 427–434

[37] Hauptmann M, Frederickx F, Struyf H, Mertens P, Heyns M, Gendt S, Glorieux C, Brems S. Enhancement of cavitation activity and particle removal with pulsed high frequency ultrasound and supersaturation. Ultrason Sonochem 2013; 20: 69–76

[38] Babu VR, Areefulla SH, Mallikarjun V. Solubility and dissolution enhancement: An overview. J Pharm Res 2010; 3: 141–145

[39] Zhao D, Chang MW, Li JS, Suen W, Huang J. Investigation of ice-assisted sonication on the microstructure and chemical quality of Ganoderma lucidum spores. J Food Sci 2014; 79: E2253–E2265

[40] Maiuolo J, Maretta A, Gliozzi M, Musolino V, Carresi C, Bosco F, Mollace R, Scarano F, Palma E, Scicchitano M, Nucera S, Sergi D, Muscoli S, Gratteri S, Muscoli C, Mollace V. Ethanol-induced cardiomyocyte toxicity implicit autophagy and NFkB transcription factor. Pharmacol Res 2018; 133: 141–150

[41] James-Martin G, Baird DL, Hendrie GA, Bogard J, Anastasiou K, Brooker PG, Wiggins B, Williams G, Herrero M, Lawrence M, Lee AJ, Riley MD. Environmental sustainability in national food-based dietary guidelines: A global review. Lancet Planet Health 2022; 6: e977-e986

[42] Ayyalasomayajula N, Bandaru LJM, Chetty CS, Dixit PK, Challa S. Mitochondria-mediated moderation of apoptosis by EGCG in cytotoxic neuronal cells induced by lead (Pb) and amyloid peptides. Biol Trace Elem Res 2022; 200: 3582–3593

[43] Ibrahim IM, Abdelmalek DH, Elfiky AA. GRP78: A cell's response to stress. Life Sci 2019; 226: 156–163

[44] Maiuolo J, Macrì R, Bava I, Gliozzi M, Musolino V, Nucera S, Carresi C, Scicchitano M, Bosco F, Scarano F, Palma E, Gratteri S, Mollace V. Myelin disturbances produced by sub-toxic concentration of heavy metals: The role of oligodendrocyte dysfunction. Int J Mol Sci 2019; 20: 4554

[45] Zhao H, Pan X. Mitochondrial Ca(2+) and cell cycle regulation. Int Rev Cell Mol Biol 2021; 362: 171–207

[46] Brini M, Calì T, Ottolini D, Carafoli E. Neuronal calcium signaling: Function and dysfunction. Cell Mol Life Sci 2014; 71: 2787–2814

[47] Maiuolo J, Gliozzi M, Musolino V, Carresi C, Nucera S, Scicchitano M, Scarano F, Bosco F, Oppedisano F, Macrì R, Mollace V. Environmental and nutritional "stressors" and oligodendrocyte dysfunction: Role of mitochondrial and endoplasmatic reticulum impairment. Biomedicines 2020; 8: 553

[48] Oppedisano F, Maiuolo J, Gliozzi M, Musolino V, Carresi C, Nucera S, Scicchitano M, Scarano F, Bosco F, Macrì R, Ruga S, Zito MC, Palma E, Muscoli C, Mollace V. The potential for natural antioxidant supplementation in the early stages of neurodegenerative disorders. Int J Mol Sci 2020; 21: 2618

[49] Di Lorenzo C, Colombo F, Biella S, Stockley C, Restani P. Polyphenols and human health: The role of bioavailability. Nutrients 2021; 13: 273

[50] Ohnishi M, Morishita H, Iwahashi H, Shitzuo T, Yoshiaki S, Kimura M, Kido R. Inhibitory effects of chlorogenic acid on linoleic acid peroxidation and hemolysis. Phytochemistry 1994; 36: 579–583

[51] Oyaizu M. Studies on products of browning reaction: Antioxidative activities of products of browning reaction prepared from glucosamine. Jpn J Nutr Diet 1986; 44: 307–315

[52] Chou TC, Martin N (Eds.). CompuSyn for Drug Combinations: PC Software and User's Guide: A Computer Program for Quantitation of Synergism and Antagonism in Drug Combinations, and the Determination of IC50 and ED50 and LD50 Values. Paramus, NJ: ComboSyn Inc; 2005